Measurements of Bi_2Te_3 Nanowire Thermal Conductivity and Seebeck Coefficient

Deyu Li[1], Amy Lucia Prieto[2], Yiying Wu[2], Marisol S. Martin-Gonzalez[2], Angelica Stacy[2], Timothy Sands[3], Ronald Gronsky[3], Peidong Yang[2], and Arun Majumdar[1]

[1]Department of Mechanical Engineering, University of California, Berkeley
[2]Department of Chemistry, University of California, Berkeley
[3]Department of Materials Science and Engineering, University of California, Berkeley

Abstract

Theoretical predictions suggest that the thermoelectric properties of nanowires could be greatly enhanced compared with the bulk materials. To investigate these predictions, bismuth telluride nanowires are synthesized by electrodeposition into the cavities of porous alumina templates. Individual nanowires are then isolated, and subjected to measurements of both thermal conductivity and Seebeck coefficient over temperatures ranging from 20 K to 320 K. All measurements are made using a microfabricated device consisting of two suspended membranes with integrated heaters and resistance thermometers. Platinum or carbon films are locally deposited at the wire and the heater pad junctions to enhance the contact conductance. Results show that the thermal conductivity of the measured Bi_2Te_3 nanowires varies from wire to wire and show different temperature dependence, probably because the wire composition and crystal structure are not the same.

Introduction

One-dimensional (1D) materials such as various kinds of nanowires and nanotubes have attracted considerable attention recently because of their potential applications in nanoelectronic and energy conversion devices [1-3]. In Ref. [4], Dresselhaus *et al.* predicted that as the diameter of a Bi nanowire scaled down below 10 nm, its thermoelectric figure-of-merit would increase significantly compared with bulk materials, which may greatly improve the performance of nanowire-based thermoelectric devices. Different techniques of fabricating various kinds of nanowires have been achieved in the past few years. For example, by pressure injecting Bi liquid melt [5] and by electrochemically depositing Bi_2Te_3 [6] into the nanochannels of anodic alumina template, single crystalline Bi nanowires and polycrystalline Bi_2Te_3 nanowires were synthesized, respectively. With vapor-liquid-solid growth method, single crystalline Si, Ge, Si/SiGe nanowires have been synthesized [7]. However, the properties of these nanowires have not been thoroughly studied yet.

In the present work, we applied a microdevice to experimentally measure the thermal conductivity and the Seebeck coefficient of individual electrodeposition fabricated Bi_2Te_3 nanowires from 20 K to 320 K. The results show that the thermal conductivity varies from wire to wire and show different temperature dependence, possibly because of the synthesis condition changes during sample preparation.

Device Fabrication, Sample Preparation, and Experimental Setup

Figure 1 shows a scanning electron micrograph (SEM) of the current design of the microdevice. It consists of two silicon nitride (SiN_x) membranes each suspended by five SiN_x beams that are more than 400 μm long. A thin Pt resistance thermometer coil and a separate Pt electrode are patterned on each membrane. Each Pt resistor could serve as a heater to increase the temperature of the suspended island. These resistors are electrically connected to contact pads by the metal lines on the suspending legs. Since the resistance of the Pt resistor changes with temperature, it also serves as a thermometer to measure the temperature of each island.

To fabricate the device, a 0.5~0.7 μm thick low stress SiN_x film is first deposited on a (100) Si wafer using low pressure chemical vapor deposition (LPCVD) method. A layer of thin Pt film (~30 nm) is then deposited on the SiN_x film by sputtering. The Pt film is patterned by photolithography using a GCA 6200 10× wafer stepper to make 200 nm to 300 nm wide Pt heater coils. After the heater coils are etched with an ion milling method, the SiN_x film is patterned and etched in a reactive ion etcher (RIE). With the patterned SiN_x film as a mask layer, the silicon substrate underneath is anisotropically etched in 10% tetramethyl ammonium hydroxide (TMAH) to about 150 μm deep. Then the two SiN_x membranes are released and suspended.

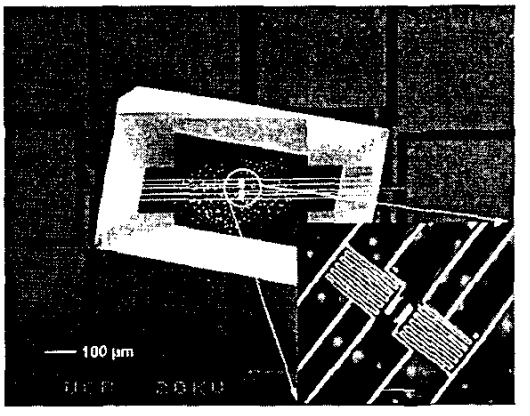

Figure 1. A scanning electron microscopy (SEM) image of the suspended heater structure. The lower insert is a higher magnification image of the two suspended membranes. The scale bar in the insert represents 10 μm.

The Bi_2Te_3 nanowires were synthesized by electrochemically filling anodized porous alumina templates. The pore diameter could be as small as 20 nm and the depth of the pores could be as large as 50 μm. For the present work, commercially available Whatman filters with a nominal 200 nm diameter pore size were used as the templates. The

0-7803-7683-8/02/$17.00

synthesized Bi_2Te_3 nanowire is polycrystalline of very small grain size (<50 nm).

The nanowires were placed on the device and bridged the two suspended membranes by solution drop-dry from an aqueous solution. For this method, the template was first dissolved and then the nanowires were dispersed into isoproponal solvent by sonication and dropped onto the suspended heater devices. After drying the solvent, we found that a nanowire was often bridging the two adjacent heater pads. In order to reduce the thermal contact resistance between the nanowire and the Pt heaters, amorphous carbon or Pt films were locally deposited at the nanowire-heater pad junctions with a scanning electron microscope or a focused ion beam (FIB). If the SEM chamber is not ultra clean, when a spot is examined with ultra high magnification (>200,000), the highly focused electron current will react with the residue organic vapor in the chamber and a thin film of amorphous carbon can be deposited locally at the focus spot. A SEM image of a Bi_2Te_3 nanowire with a diameter of 360 nm bridging the two suspended heater pads is shown in Figure 2a. Focused ion beam is another option to enhance the nanowire-heater pad contacts. In a focused ion beam, Pt or W containing organometalic precursor is heated up and injected in vapor form from a needle to a local region where it reacts with the energetic ions. As a result, Pt or W films are locally deposited at a designated region. Figure 2b shows a 391 nm Bi_2Te_3 nanowire bridging the two heater pads with 800 nm thick Pt films deposited locally at the nanowire-heater pad junctions.

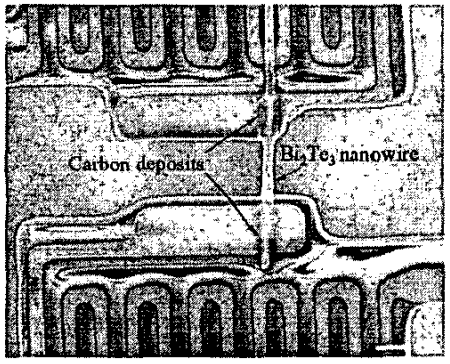

(a)

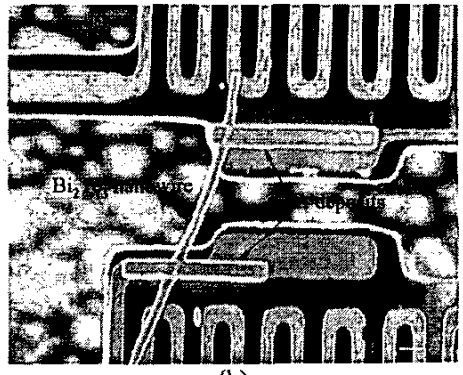

(b)

Figure 2. SEM images of Bi_2Te_3 nanowires bridging the two suspended heater pads. The scale bars represent 1 μm. (a) a 360 nm nanowire with amorphous carbon deposits at contacts. (b) a 391 nm nanowire with Pt deposits at contacts.

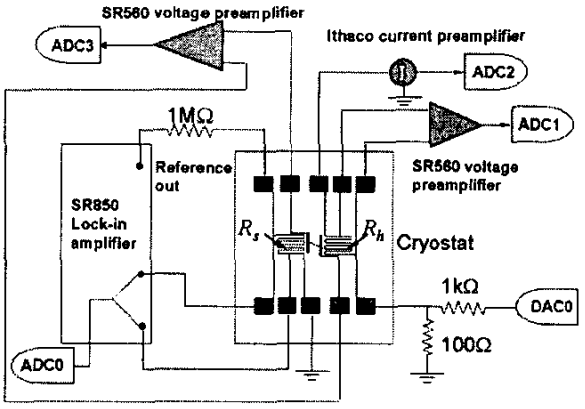

Figure 3. Schematic diagram of the experimental set-up

Once the device and the sample were prepared, they were placed into a cryostat (Janis CCS-250) with a temperature range from 10 K to 320 K. During the experiment, the vacuum level in the cryostat was kept at ~2×10^{-6} Torr. To a very accurate approximation, the heat conduction through the nanowire is the only thermal path between the two suspended heater islands. The electronics for the experiment is shown in Figure 3. All the data acquisition was implemented with a National Instruments (NI) data acquisition board (DAC and ADC in the figure represent the digital to analog and analog to digital channels). A bias voltage applied to one of the resistors, R_h, creates Joule heat and increases the temperature, T_h, of the heater island from the thermal bath temperature, T_0. Under steady state, part of the heat will transfer through the nanowire to the other resistor, R_s, and raise its temperature, T_s. Solving the heat transfer equations of the system, denoting the thermal conductance of the wire, G_w, and the suspending legs, G_l, we have,

$$T_h = T_0 + \frac{G_l + G_w}{G_l(G_l + 2G_w)}P, \text{ and } T_s = T_0 + \frac{G_w}{G_l(G_l + 2G_w)}P,$$

where P is the power dissipated on the resistor, R_h. More details could be found in [8]. With the measured wire diameter and length, the thermal conductivity of the nanowires could be easily derived. Since the two pads are at different temperatures, for thermoelectric materials such as Bi_2Te_3, we can measure the voltage difference across the wire with the two extra electrodes and derive the Seebeck coefficient $S = \Delta V/\Delta T$.

Results and Discussions

The same techniques have been applied to measure multi-walled carbon nanotubes (MWCNTs) [8] and single crystalline silicon nanowires [9] and Si/SiGe superlattice nanaowires [10]. The results on these nanotubes and nanowires show expected temperature dependence and fit the

theoretical predictions quite well. However, the measurements on the Bi_2Te_3 nanowires show quite unexpected results and different results were obtained for different samples. Figure 4a shows the measured thermal conductivities for 228, 360, and 391 nm diameter Bi_2Te_3 nanowires. The bulk Bi_2Te_3 thermal conductivity data [11] are also shown for comparison. Figure 4b shows the measured thermoelectric power for the 391 nm diameter wire.

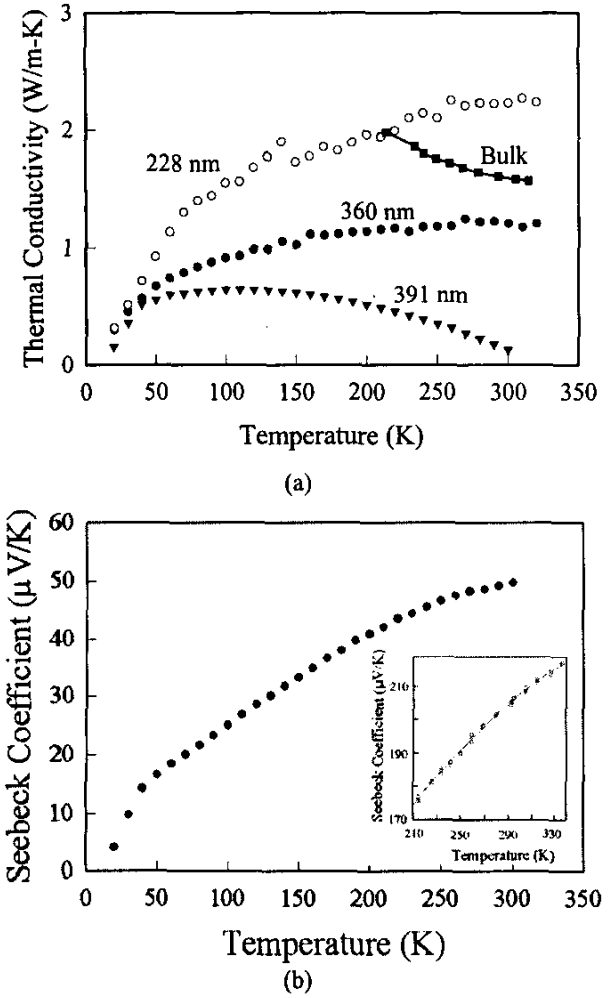

Figure 4. (a) Thermal conductivities of 228, 360, and 391 nm diameter Bi_2Te_3 nanowires. Bulk data from Ref. [11] are also shown for comparison. (b) Seebeck coefficient of the 391 nm Bi_2Te_3 nanowire. The optimally doped bulk values (from Ref. [11]) are shown in the insert for comparison.

The measured thermal conductivities for the 228 and 360 nm diameter Bi_2Te_3 nanowires increase monotonically from 20 K to 320 K, while the thermal conductivity for the 391 nm wire first increases with temperature to about 110 K, and then decreases with increasing temperature. The measured value of the 228 nm wire is about twice that of the 360 nm wire and is about 2.2 W/m-K at room temperature, which is even higher than the bulk value. The measured thermal conductivity for the 391 nm wire at room temperature is about 0.13 W/m-K, which is about 10 times smaller than the bulk value. The measured thermoelectric power shows the same trend as the bulk Bi_2Te_3 material, as can be seen in the insert of Figure 4b. Since the nanowire is not intentionally doped, the thermoelectric power is lower than the optimally doped bulk material.

Since this measurement technique has been used previously and obtained reasonable results for MWCNTs and Si nanowires, it seems likely that the discrepancies for the Bi_2Te_3 nanowire lie in the sample preparation. The only difference in the measurements is that for the 391 nm diameter Bi_2Te_3 nanowire, the wire-heater pads contacts are enhanced with Pt by FIB, while for all the other measurements, the contacts are enhanced with carbon by SEM.

The templates used for the nanowire synthesis are commercially available Whatman filters with nominal pore diameters of 200 nm. The top view and the side view of Whatman filters are shown in Figure 5. From the SEM images, it is clear that the pore size is not uniform and even for the same pore, its size varies along the axial direction. The measured Bi_2Te_3 nanowire diameters also verify that the pore size is not uniform. Since the diffusion of Bi and Te ions should be different for different diameter pores, it is possible that the deposition conditions change in the synthesis process as the pore diameter changes and resulting in Bi_2Te_3 nanowires of different composition and crystalline structure.

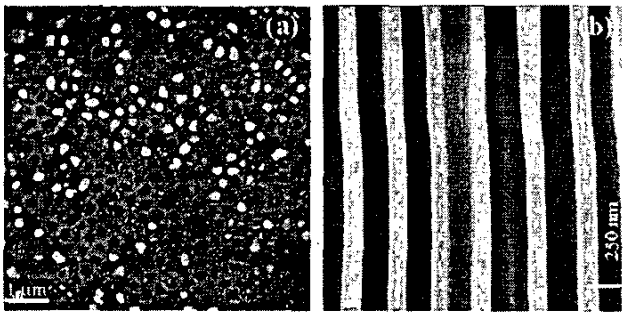

Figure 5. SEM images of the top view (a) and side view (b) of the Whatman filter templates. The scale bar in (a) represents 1 μm and the scale bar in (b) represents 250 nm. The white spots in (a) are filled Bi_2Te_3 nanowires.

The second possible reason for the unexpected results is that the nanowire contains elements other than Bi and Te. Figure 6 shows the energy dispersive X-ray spectroscopy (EDX) results on one wire starting from the bottom of a Bi_2Te_3 nanowire. These data show that for the first 1.8 μm, the wire is in fact silver telluride. The silver comes from the sputtered silver that is used as the electrode for the electrodeposition. After the first 2 μm, there is still some silver residue present. The EDX results also indicate that the wires contain a large fraction (5-10%) of phosphorous, which likely comes from the pore etching acid for the template fabrication. However, it is also possible that the phosphorous is from some phosphate that just adheres to the outside of the nanowire. The temperature dependence of the thermal conductivity for the 228 nm and 360 nm Bi_2Te_3 nanowires

does not show any Umklapp scattering, but shows similar temperature dependence as alloys, which may come from the silver and phosphorous present in the wires.

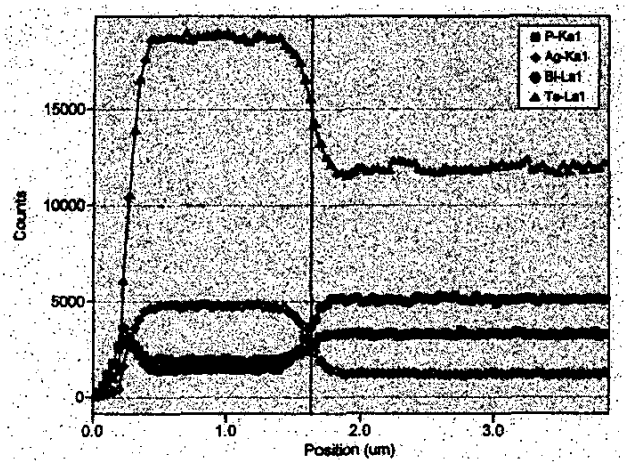

Figure 6. Energy dispersive X-ray spectroscopy (EDX) results starting from the bottom of a Bi2Te3 nanowire.

It is interesting that the measured thermal conductivity of the 391 nm Bi_2Te_3 nanowire is an order of magnitude lower than bulk Bi_2Te_3 value at room temperature. At the same time, the temperature dependence of the nanowire is similar to that of a bulk sample. As mentioned previously the only difference between the measurement of this nanowire and all other measurements is that for this wire the contact is enhanced with Pt deposited by the FIB instead of carbon deposited by the SEM. The possibility that the FIB has some unknown effects on the nanowire still cannot be ruled out at this time. Another possibility is that this wire came from the top half of the template and does not contain any silver, while the other two wires may have come from the bottom and were contaminated with silver from the electrode. It is also possible that this wire does not have any phosphorous contamination while the other two have. The fact that the thermal conductivity decreases with increasing temperature for the nanowire with the 391 nm diameter seems to indicate that phonon-phonon Umklapp scattering has a greater influence than any alloy scattering. The lack of alloy scattering is another indication that this wire may not contain much silver or other contaminants. The fact that the thermal conductivity is so low, yet Umklapp scattering is still present is really puzzling. One possible reason for the extremely low conductivity is that this particular nanowire is highly polycrystalline with a very small grain size. However, it would then seem likely that the scattering at the grain boundaries would dominate and the effects of any Umklapp scattering would not be visible. Further work is required to confirm and fully explain these results.

Summary

Thermal conductivities and Seebeck coefficient of electrodeposition synthesized Bi_2Te_3 nanowires have been measured. The thermal conductivities of different wires show different values and different temperature dependence, probably because of the sample is not of the same composition and crystalline structure. However, at this stage, it is hard to draw solid conclusions from the current results. Further efforts such as improve the device design to make it ready for the TEM and X-ray diffraction examination on the measured wire will be carried out. More measurements on the well-characterized Bi_2Te_3 nanowire samples will be done.

Acknowledgements

The authors wish to thank Dr. P. Kim, Dr. L. Shi, and Dr. S. Huxtable for helpful discussions and acknowledge the support from NSF and DOE.

References

1. Collins, P. G. *et al*, "Nanoscale Electronic Devices on Carbon Nanotubes," *Nanotechnology*, Vol. 9 (1998), pp. 153-157.
2. Cui, Y. *et al*, "Functional nanoscale Electronic Devices Assembled Using Silicon Nanowire Building Blocks," *Science*, Vol. 291 (2001), pp. 851-853.
3. Dresselhaus, M. S. *et al*, "Quantum Wells and Quantum Wires for Potential Thermoelectric Applications," *Semiconductors and Semimetals*, Vol. 71 (2001), pp. 1-121.
4. Dresselhaus, M. S. *et al*, "Low-dimensional thermoelectric materials," *Phys. Solid State* Vol. 41, No. 5 (1999), pp. 679-682.
5. Zhang, Z. *et al*, "Processing and Characterization of Single-Crystalline Ultrafine Bismuth Nanowires," *Chem. Mater.*, Vol. 11 (1999), pp. 1659-1665.
6. Prieto, A. L. *et al*, "Electrodeposition of Ordered Bi_2Te_3 Nanowire Arrays," *J. Am. Chem. Soc.*, Vol. 123 (2001), pp. 7160-7161.
7. Wu, Y. *et al*, "Inorganic Semiconductor Nanowires: Rational Growth, Assembly, and Novel Properties," *Chem. Eur. J.*, Vol. 8, No. 6 (2002), pp. 1261-1268.
8. Kim, P. *et al*, "Thermal Transport Measurements of Individual Multiwalled Nanotubes," *Phy. Rev. Lett.*, Vol. 87 (2001), 215502-1.
9. Li, D. *et al*, "Thermal Conductivity of Individual Silicon Nanowires," (In preparation, will submit to *Phy. Rev. Lett.*).
10. Li, D. *et al*, "Thermal Conductivity of Si/SiGe Superlattice Nanowires," (In preparation, will submit to *Appl. Phy. Lett.*).
11. Rowe, D. M., CRC Handbook of Thermoelectrics CRC Press (1995).